Separation Science and Technology
Publication details, including instructions for authors and subscription information:
http://www.informaworld.com/smpp/title~content=t713708471

Optimization of Transport-Driven Continuous SPLITT Fractionation

J. Calvin Giddings[a]
[a] FIELD-FLOW FRACTIONATION RESEARCH CENTER, DEPARTMENT OF CHEMISTRY, UNIVERSITY OF UTAH SALT LAKE CITY, UTAH

To cite this Article Giddings, J. Calvin(1992) 'Optimization of Transport-Driven Continuous SPLITT Fractionation', Separation Science and Technology, 27: 11, 1489 — 1504
To link to this Article: DOI: 10.1080/01496399208019438
URL: http://dx.doi.org/10.1080/01496399208019438

SEPARATION SCIENCE AND TECHNOLOGY, 27(11), pp. 1489–1504, 1992

Optimization of Transport-Driven Continuous SPLITT Fractionation

J. CALVIN GIDDINGS
FIELD-FLOW FRACTIONATION RESEARCH CENTER
DEPARTMENT OF CHEMISTRY
UNIVERSITY OF UTAH
SALT LAKE CITY, UTAH 84112

Abstract

Continuous SPLITT fractionation (CSF) utilizes various forces acting across the thin dimension of a ribbonlike flow channel or cell to segregate suspended particles and macromolecules into different flow laminae. One or more splitters at the outlet of the channel then divide the differentially populated laminae into two or more substreams. The separation is rapid because of the extreme thinness (usually <0.5 mm) of the cell. The throughput/cell volume ratio is high because of the high separation speed. The purpose of this paper is to examine factors affecting resolution, speed, and throughput in transport-based CSF. The time of separation is roughly proportional to the path length of separation, giving CSF a $>10^2$-fold advantage over many conventional techniques like gravitational sedimentation. The resolving power of CSF is related to the ratio of inlet substream flow rates, making possible the direct control of resolution. A straightforward tradeoff is found between resolution and throughput. The throughput is shown to be proportional to the concentration of particles in the feed stream, to the field strength, to the mobility range that can be tolerated for incompletely resolved material, and to the SPLITT cell area. However, throughput is independent of cell thickness. Optimization considerations suggest the desirability of working with very thin cells of high area and thus a high aspect ratio in CSF.

INTRODUCTION

Split-flow thin cells, or SPLITT cells, are devices that make possible the continuous and rapid fractionation of constituents that can be differentially transported by the application of an externally imposed field or gradient (*1–3*). Electrically charged species (such as proteins) subject to electrical field displacement and particles subject to gravitational or centrifugal displacement are particularly good candidates for SPLITT separation. The separation process itself is termed continuous SPLITT fractionation (CSF).

SPLITT cells are thin ribbonlike channels having flow splitters at one or both ends. An edge view of a typical cell is shown in Fig. 1. (The thickness, w, of the cell is exaggerated for purposes of illustration.) By adjusting the relative flow rates of the substreams entering inlets a' and b', the position of the inlet splitting plane (ISP) dividing the two incoming substreams can be adjusted as required (*1*). Most often the ISP is forced by a large b' flow (consisting of inert liquid) to a position near wall A, which compresses feed substream a' into a thin lamina containing the mixture to be separated. The thinner the resulting feed lamina, the higher the resolution achievable. Particles of different size, mass, charge, etc. are then driven by the applied field at different velocities toward wall B. Those mobile enough to cross the outlet splitting plane (OSP), dividing the two outlet substreams, are collected from outlet b; the remainder emerge at outlet a.

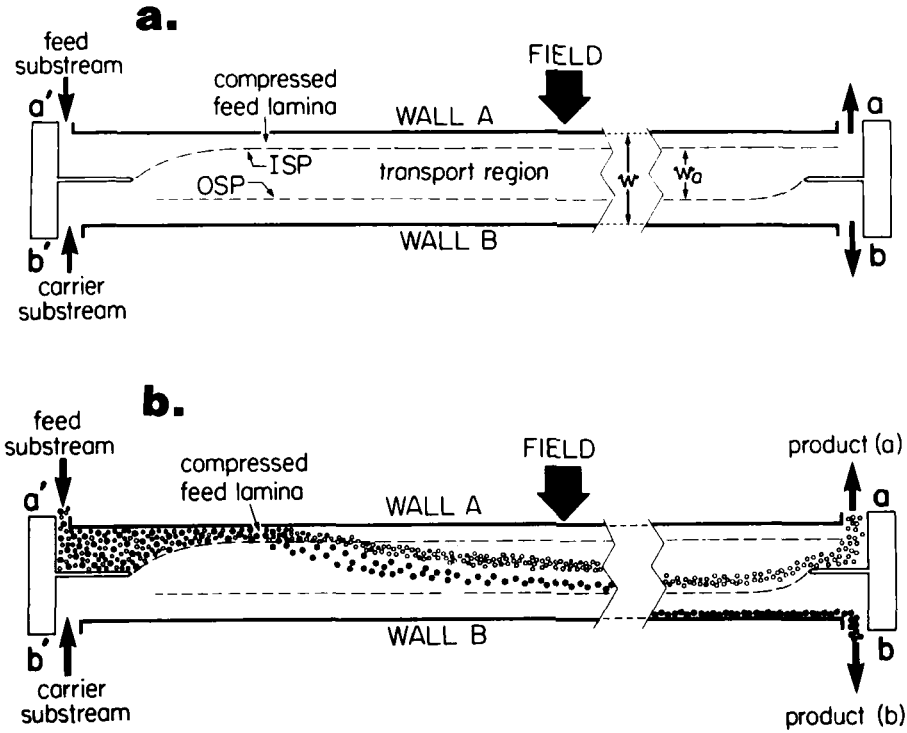

FIG. 1. Configuration (edge view) of SPLITT cell and separation of two monodisperse particle populations entering SPLITT cell in substream a'.

The separation described above is based on differences in transport rates. [Transport-based separation in SPLITT cells can also be driven by diffusion (*1*, *4*) or hydrodynamic lift forces (*5*), but these forms of transport are not treated here.] If different particles are driven to different final positions (e.g., toward different walls), then the separation is equilibrium based (*1*, *3*).

Whether separated in the transport or equilibrium mode, particles need only be transported over a very short path, scaled to the thickness of the SPLITT cell, to achieve separation. Thus separation is intrinsically rapid, often completed in less than 1 minute.

Most often the thickness w of a SPLITT cell is <1 mm; it may range down to 100 μm or less. The side-to-side breadth b is generally >50 times w. Thus, except for the two narrow edge regions, the flow is uniformly parabolic between walls A and B. Consequently all particles (except for the small fraction near the edges) entering at the same elevation are subjected to exactly the same flow displacements. Remarkably high resolution can thus be achieved, although it is subject to certain tradeoffs to be described below.

Many variables affect the efficacy of SPLITT operation (*1*). Among the principal variables are various cell dimensions, fixed when the cell is assembled, and the flow rates of the multiple inlet and outlet substreams, subject to flexible adjustment to meet different separative requirements. The field strength is also adjustable. (If the system is designed specifically to utilize gravity, an adjustment in angle of tilt can produce a variable field strength limited to the range from zero to 1 gravity.) The purpose of this paper is to show how changes in these variables affect throughput, resolution, speed, and material recovery, and to propose strategies for the manipulation of these variables that will lead to a closer approach to separative goals.

SEPARATION SPEED AND RESOLUTION IN SPLITT CELLS

We have noted that separation in a SPLITT cell is rapid as a result of the short transport path. Specifically, the time required for particles migrating at velocity U to traverse the transport region of thickness w_t is

$$t = w_t/U \tag{1}$$

Velocity U can be replaced by the product of field strength S and generalized mobility m, giving

$$t = w_t/mS \tag{2}$$

For sedimentation transport, S is measured as acceleration G (e.g., in cm/s^2) and m is the sedimentation coefficient; for electrical transport, S is the electrical field strength (V/cm) and m is the electrophoretic mobility. In either case

$$m = U/S = F/fS \tag{3}$$

where F is the force exerted on a particle and f is the particle's friction coefficient. With this m substituted back into Eq. (2), we have

$$t = w_t f/F \tag{4}$$

For spherical particles of diameter d, Stokes' law gives (*6*)

$$f = 3\pi\eta d \tag{5}$$

where η is the viscosity. For sedimentation

$$F = \frac{\pi}{6} d^3 \Delta\rho G \tag{6}$$

in which $\Delta\rho$ is the difference in the density of the particle and that of the carrier. Thus

$$t = \frac{18 w_t \eta}{\Delta\rho G d^2} \tag{7}$$

For cell-like particles having $d = 10$ μm and $\Delta\rho = 0.1$ g/mL suspended in an aqueous carrier with $\eta = 0.01$ poise and subjected to 1 gravity of acceleration, we calculate that a time of only 18 s is required to sediment across a transport region of thickness $w_t = 100$ μm. (Even less time is needed for the comparable transport of larger and denser particles as expressed clearly by Eq. 7; longer times are needed for smaller particles closer to neutral buoyancy.) By contrast, 2 h are needed for transporting the above cell-like particle over a 4-cm sedimentation cell. (More time will be needed if a density gradient is used as an anticonvectant.) Both times can, of course, be reduced by the use of centrifugal forces, but their ratio remains 1:400. (The times calculated above are those for migration through the designated transport regions. Additional time may be required in the SPLITT case to sweep particles through the remaining cell length, or in the classical sedimentation case to isolate and recover the products.)

While the above treatment illustrates the enhanced speed of transport characteristic of SPLITT cells, the theory of transport, recovery, and resolution is most simply and directly formulated in terms of constituent volumetric flow rates (*2*). In order to utilize this approach, we define the volumetric flow rates entering inlets a' and b' and exiting outlets a and b as $\dot{V}(a')$, $\dot{V}(b')$, $\dot{V}(a)$, and $\dot{V}(b)$, respectively. Because the total inlet flow must equal the total outlet flow, these flow rates are constrained by the condition

$$\dot{V}(a) + \dot{V}(b) = \dot{V}(a') + \dot{V}(b') \tag{8}$$

or

$$\dot{V}(a) - \dot{V}(a') = \dot{V}(b') - \dot{V}(b) \tag{9}$$

The volumetric flow rate $\dot{V}(t)$ coursing through the transport region between the two splitting planes (see Fig. 1) can therefore be expressed in either of two forms, as follows:

$$\dot{V}(t) = \dot{V}(a) - \dot{V}(a') = \dot{V}(b') - \dot{V}(b) \tag{10}$$

Clearly, $\dot{V}(t)$ is directly controlled by the flow rates of the entering and exiting substreams.

We have noted that high resolution in the transport mode of operation is contingent on the compression of feed substream a' into a thin lamina near wall A. Along with the requirement for a thin feed stream, high resolution based on transport (with the exception of diffusion-based transport) requires that the diffusional broadening of component bands or laminae be held within reasonable limits. The situation is analogous to that encountered in ideal zonal electrophoresis or sedimentation where the band broadening accompanying field-induced migration is diffusion controlled (*6*). The sharpness of the separation, as in chromatography, can be judged by the number N of theoretical plates generated during transport. For field-driven (SPLITT) migration, the effective N is given by the ratio of the two energies (*6*):

$$N = Fw_t/2kT \tag{11}$$

where F is the force on the particle inducing its transport, w_t is the length of the transport path, and kT is thermal energy. Since $N = (w_t/\sigma)^2$, and the standard deviation σ of a narrow pulse caused by diffusion should be no more than $0.1w_t$ for high resolution, we generally require $N \geq 10^2$. For

the cell-like particle described above (d = 10 μm, $\Delta\rho$ = 0.1 g/mL) sedimenting 100 μm under the influence of gravity, Eq. (11) (with the aid of Eq. 6) yields N = 6300, well above the desired level of 10^2. Each type of macromolecule or particle should be checked against this criterion to assure achievable resolution.

We now focus on a particular feed component entering inlet a' of the SPLITT cell of Fig. 1. The component we examine is one that reaches but only partially crosses the OSP. Thus the component lamina at the outlet straddles the OSP, part emerging from outlet a and part from outlet b. The component is therefore in the transition gap between fully resolved components. It has been shown that the fraction F_b ($1 \geq F_b \geq 0$) of such a component disgorged from outlet b is (*2*)

$$F_b = \frac{\Delta\dot{V} - \dot{V}(t)}{\dot{V}(a')} = \frac{\Delta\dot{V} + \dot{V}(a') - \dot{V}(a)}{\dot{V}(a')} \tag{12}$$

providing $\dot{V}(a) \geq \Delta\dot{V} \geq \dot{V}(a) - \dot{V}(a')$, where $\Delta\dot{V}$ is the volumetric flow rate of the ribbon of fluid that the component particles traverse due to field-induced migration. The quantity $\Delta\dot{V}$ is given generally by (*2*)

$$\Delta\dot{V} = bLU = bLmS \tag{13}$$

where b is the breadth and L is the length of the cell (and thus bL is the working area of the cell in the plane perpendicular to the field). As above, U is the velocity of the field-induced migration, equal to the product of the generalized mobility m and the field strength S.

If we substitute Eq. (13) into Eq. (12) and solve for m, we get

$$m = \frac{F_b\dot{V}(a') + \dot{V}(a) - \dot{V}(a')}{bLS} \tag{14}$$

which specifies the mobility of the particles that will be collected from outlet b at fractional level F_b, given the experimentally realized values of flow rates, field strength S, and cell area bL. We note that $\dot{V}(a) - \dot{V}(a')$ equals the flow rate $\dot{V}(t)$ of the transport region occupying the space between the splitting planes (see Eq. 10).

The mobility m_1 of particles just barely mobile enough to be *fully* collected at outlet b is obtained from Eq. (14) by setting F_b = 1:

$$m_1 = \dot{V}(a)/bLS \tag{15}$$

Clearly, the fraction F_a exiting port a is reduced to zero when m reaches m_1 since

$$F_a + F_b = 1 \tag{16}$$

As the mobility decreases below m_1, F_b will decrease and F_a will correspondingly increase. At a certain mobility level, $m = m_0$, F_b reaches zero, and F_a becomes unity. From Eq. (14):

$$m_0 = \frac{\dot{V}(a) - \dot{V}(a')}{bLS} = \frac{\dot{V}(t)}{bLS} \tag{17}$$

The mobility range between m_0 and m_1 is that for which feed particles divide between outlets a and b. Thus particles having mobilities falling in this interval, whose range is

$$\Delta m = m_1 - m_0 = \dot{V}(a')/bLS \tag{18}$$

are not fully separated from any other particle fraction. The way in which a broad particle population divides between outlets a and b both within and outside of this unresolved range is shown in Fig. 2.

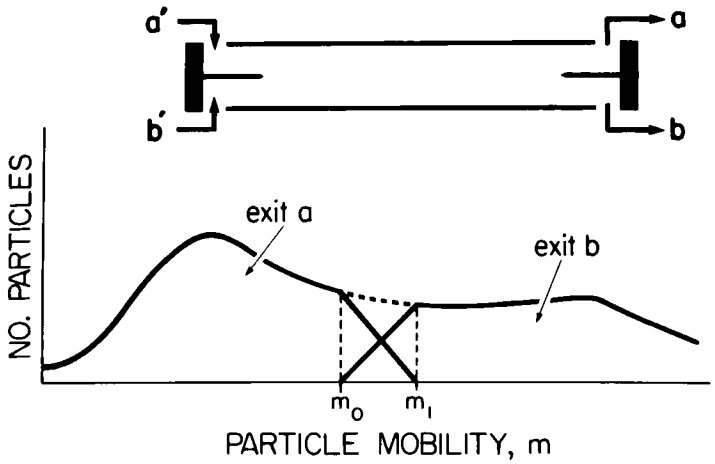

FIG. 2. Arbitrary particle distribution curve plotted along mobility (m) axis. The fractions collected from outlets a and b are shown.

We can relate F_b to m, m_0, and m_1 if we substitute Eq. (13) into Eq. (12) and (with the help of Eq. 10) rearrange the latter into the form

$$F_b = \frac{m - \dfrac{\dot{V}(t)}{bLS}}{\dfrac{\dot{V}(a')}{bLS}} \tag{19}$$

A comparison with Eqs. (17) and (18) shows that this expression reduces to

$$F_b = \frac{m - m_0}{\Delta m} = \frac{m - m_0}{m_1 - m_0} \tag{20}$$

which is applicable in the range $m_1 \geq m \geq m_0$. This expression shows that F_b increases linearly with m over the unresolved range Δm.

A measure of the relative breadth (and thus negative impact) of the unresolved region can be formulated as $\Delta m/m_1$. From Eqs. (15) and (18) we get for this index

$$\Delta m/m_1 = \dot{V}(a')/\dot{V}(a) \tag{21}$$

For the comparable index $\Delta m/\overline{m}$, where $\overline{m}$ is the mobility in the center of the unresolved region (for which $F_b = F_a = 0.5$), we obtain

$$\frac{\Delta m}{m} = \frac{2\dot{V}(a')}{2\dot{V}(a) - \dot{V}(a')} \tag{22}$$

The resolving power of the system can be expressed as either $m_1/\Delta m$ or $\overline{m}/\Delta m$, the latter given by

$$\frac{\overline{m}}{\Delta m} = \frac{2\dot{V}(a) - \dot{V}(a')}{2\dot{V}(a')} = \frac{\dot{V}(a)}{\dot{V}(a')} - \frac{1}{2} \tag{23}$$

whereas $m_1/\Delta m$ is given by the simple ratio

$$m_1/\Delta m = \dot{V}(a)/\dot{V}(a') \tag{24}$$

If, for example, $\dot{V}(a)$ is 10 times $\dot{V}(a')$, $m_1/\Delta m = 10$ and $\overline{m}/\Delta m = 9.5$; if $\dot{V}(a) = 5\dot{V}(a')$, $m_1/\Delta m = 5$ and $\overline{m}/\Delta m = 4.5$.

Since $m = d^2\Delta\rho/18\eta$ (see Eqs. 3, 5, and 6) for sedimenting particles, the resolving power expressed in terms of d is nearly twice as high as that written above. Specifically we obtain

$$\frac{d_1}{\Delta d} = \frac{2m_1}{\Delta m}\left[\frac{1}{2}\left(1 + \left(\frac{m_0}{m_1}\right)^{1/2}\right)\right] \cong \frac{2m_1}{\Delta m} \tag{25}$$

or

$$d_1/\Delta d \cong 2\dot{V}(a)/\dot{V}(a') \tag{26}$$

The above equations yield an idealized resolution that may, in practice, not be reached. However, it may also be exceeded. A failure to reach the designated resolution levels may be due to imperfections in the splitter, which must accurately divide the few-hundred-micron thick space of the several-centimeter broad channel into even entry and exit slits. Any misalignment of the splitters will cause a degradation in resolution. In addition, diffusion will cause some resolution loss as noted above; in most practical cases this loss is of minor importance. A slight degradation will arise also due to the reduction in flow velocity in the edge regions, which will allow a few lower mobility particles that normally exit a to exit b instead. However, all high mobility particles should exit b without exception.

Rather surprisingly, there are significant factors that may lead to a sharpening of the resolution to a level substantially better than that predicted above. These resolution enhancement factors fall into three categories: finite particle size effects, the influence of hydrodynamic lift forces, and transport effects in the splitter region. The enhancement of resolution for all of these effects can be understood in relationship to Fig. 3 and the following discussion.

In describing the distribution of material (represented by F_b) emerging from the two outlets a and b between the upper and lower bounds of mobility, m_1 and m_0, respectively, that define the incompletely resolved portion of a material subjected to fractionation under specific experimental conditions, we have tacitly assumed (based on the theory developed in Ref. 2) that the particles entering in feed substream a' are evenly distributed over the compressed lamina lying above the inlet splitting plane as shown in Fig. 1. The particles whose center of gravity initially lies next to wall A require a mobility of m_1 to realize displacement to the outlet splitting plane during flow displacement in the cell. Particles whose centers of gravity are originally found at the inlet splitting plane (immediately adjacent to the splitter) need only have mobility m_0 to reach the outlet splitting plane. These two extremes in starting positions define the region of incomplete resolution between m_0 and m_1. However, the center of gravity of a particle

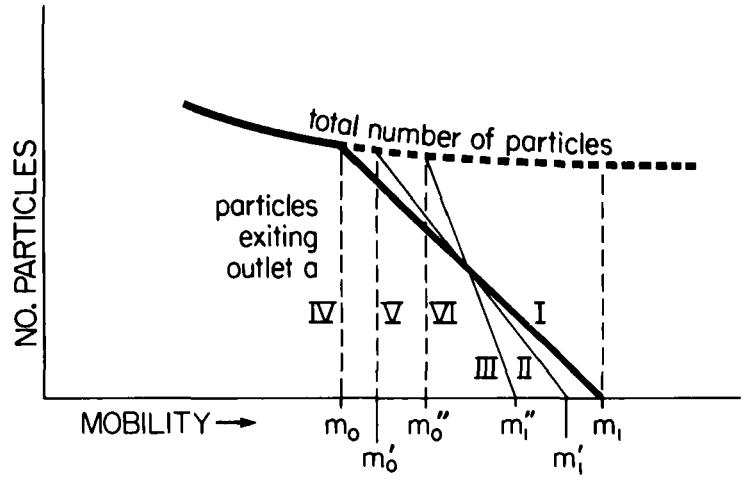

FIG. 3. Magnification of incompletely resolved region of Fig. 2 showing other mobilities that may form resolution boundaries. See text for explanation.

of finite size cannot lie against wall A; it can lie no closer to the wall than one radius due to steric exclusion. A particle removed one radius from the wall need not have mobility m_1 to reach the outlet splitting plane; because of its head start, a slightly smaller mobility m_1' will suffice. Likewise, the particles having the smallest possible mobility consistent with reaching the outlet splitting plane do not begin their field-driven transport at the inlet splitting plane. Instead, their centers of gravity will lie above the inlet splitting plane due to the fact that their finite size keeps them elevated above the splitter before entering the separation chamber. The increase in mobility that these particles need to reach the outlet splitting plane due to steric effects is represented by an increase from m_0 to m_0'. Thus steric effects dictate that a slightly narrowed range of mobilities, from m_0' to m_1', corresponds to incompletely resolved material as opposed to the range from m_0 to m_1 that would be applicable without steric effects. Thus Line I in Fig. 3, representing the recovery of particles of a given mobility from outlet a, becomes somewhat steeper (Line II) under the influence of steric effects.

Even more resolution enhancement will be gained from lift forces in the system. Particles starting near any surface will not remain in close contact with that surface but, due to hydrodynamic lift forces, will be driven away from the surface during flow displacement. The degree to which particles are removed from the immediate vicinity of the walls depends upon the shear rate of the fluid flowing near these confining surfaces (7). These lift forces further confine the range of mobilities corresponding to incompletely

resolved material. In Fig. 3 this range is shown to extend from m_0'' to m_1'' with Line III showing the recovery of the particulate material from outlet port a.

The other factor that plays a role in resolution enhancement is a result of the field-induced transport experienced by the particles while still in the splitter region near the inlet. In most situations, particles will begin their displacement toward wall B as soon as they first enter inlet a'. However, their path is temporarily impeded by the presence of the splitter. Consequently, particles will begin to accumulate near the splitter surface, all the while being displaced downstream from the inlet (splitter) region toward the main separation chamber. If the inlet splitter is sufficiently long, all the particles (or at least all that are candidates to reach the outlet splitting plane) may reach the splitter surface. In this case the particles could, in theory, enter the separation chamber confined in a narrow band of streamplanes immediately above the inlet splitting plane. If one did not encounter perturbations due to the increased particle concentration in this thin laminar layer, the particles would, in principle, divide rather sharply around mobility m_0. The partitioning line between the two outlets would then be the vertical Line IV. For finite-sized particles, whose centers of gravity would enter the separation chamber somewhat above the inlet splitting plane, particles would be divided relatively sharply around mobility m_0' and thus partitioned according to vertical Line V. Hydrodynamic lift forces would displace these features to the right, corresponding to mobility m_0'' and partitioning Line VI.

The above preliminary discussion shows that various resolution enhancing factors have a significant potential for improving SPLITT performance. These factors are likely to work most beneficially in SPLITT cells in which the flow space on the feed side of the inlet splitter is sufficiently long to accommodate the required transport (and perhaps thin enough to realize finite particle size and lift effects). A good deal more theoretical and experimental work is needed to clarify the practical implications of these factors. In the theoretical treatment below, these factors are neglected.

THROUGHPUT

The success of a continuous separation system depends strongly on both material throughput and resolving power. The throughput is clearly proportional to the volumetric flow rate $\dot{V}(a')$ of the feed input substream a'. More precisely, the throughput can be expressed as

$$\mathrm{TP} = \phi \dot{V}(a') \tag{27}$$

which gives the volume of feed material processed per unit time, with ϕ equal to the volume fraction of the material of interest in substream a'.

Equation (27), in combination with Eq. (23) or (24), shows that an inherent tradeoff exists between throughput and resolving power. As $\dot{V}(a')$ is increased to augment throughput, the resolving power expressed by Eq. (24) becomes smaller.

Our approach below to the optimization of separation is based on the assumption that some minimum resolving power must be reached in order to properly process the feed stream. We then seek a maximum throughput subject to the specified constraint of the fixed resolving power.

Equation (21) constitutes a relationship between $\dot{V}(a')$ and $\dot{V}(a)$ that we can rewrite as

$$\dot{V}(a') = \dot{V}(a)\frac{\Delta m}{m_1} \tag{28}$$

where $\Delta m/m_1$ is fixed by the resolving power requirement. The value of $\dot{V}(a)$ is, in turn, fixed by the choice of the cutoff mobility m_1, above which all particles emerge from exit b. The relevant expression is $\dot{V}(a) = bLSm_1$, obtained from Eq. (15). When this is combined with Eq. (28), we have

$$\dot{V}(a') = bLS\Delta m \tag{29}$$

and the throughput, Eq. (27), becomes simply

$$\mathrm{TP} = \phi(bL)S\Delta m \tag{30}$$

In the case of sedimentation where $S = G$ and $m = d^2\Delta\rho/18\eta$, we obtain

$$\mathrm{TP} = 2\phi bLG\frac{\Delta\rho}{18\eta}\bar{d}^2\frac{\Delta d}{d} \tag{31}$$

where Δd is the difference in and $\bar{d}$ is the average of the two diameters for which $F_a = 1$ and $F_a = 0$, respectively. This expression shows that TP increases rather sharply with the mean "cutoff" diameter $\bar{d}$ at a given fractional diameter resolution $\bar{d}/\Delta d$.

Equation (30) provides a base for some general approaches to maximizing throughput. First of all, in accordance with expectations, TP increases with the volume fraction ϕ of active material in the input stream. Thus ϕ should be as high as possible, providing excessive values are not reached that will induce convective currents or significantly perturb the transverse migration rates in a way that degrades resolution. Studies of sedimentation suggest that ϕ must be limited to ~0.01 to retain a close adherence to Stokes' law (*8*). New experimental work will be required to see if that limit can be exceeded in practical applications.

With regard to cell dimensions, Eq. (30) shows that throughput is independent of cell thickness w. As pointed out previously, the benefit of the increase in channel (processing) volume with w is offset by the lengthened transport path w_t, which proportionately reduces the speed of separation (*1*). Throughput thus remains constant with these changes associated with a change in w. However, throughput is not independent of other dimensions. Equation (30) shows that throughput is proportional to cell area bL. For most existing SPLITT cells, breadth $b \approx 2$–4 cm, allowing considerable flexibility for increasing b. A cell design for further increasing b without allowing end effects to get out of hand has been proposed (*1*).

Throughput is, in particular, proportional to cell length L, which is measured as the distance between splitter edges. It has been noted that as L increases, there must be a concomitant increase in flow rates (*1*). We can illuminate this point using Eqs. (15), (17), and (18). Equation (15), for example, shows that the total flow rate exiting outlet a is

$$\dot{V}(a) = bLSm_1 \tag{32}$$

which shows that $\dot{V}(a)$ increases in proportion to L. The total channel flow is the sum

$$\dot{V} = \dot{V}(a) + \dot{V}(b) = bLSm_1 + \dot{V}(b) \tag{33}$$

where exit flow rate $\dot{V}(b)$ can be adjusted over fairly wide limits without affecting the separation much.

The foregoing equations and related expressions show that for fixed m_0 and m_1, throughput and the flow rates $\dot{V}(a')$, $\dot{V}(t)$, and $\dot{V}(a)$ are all proportional to channel length L and independent of w. Thus throughput can, in theory, be augmented by building longer cells. However, as pointed out previously, the concomitant increase in flow rates leads to the possibility of flow disturbances (*1*). Of specific concern is the increasing Reynolds number and the possible onset of turbulence which, if fully developed at any point along the cell length, would largely destroy all transport-based separation. This concern is addressed below.

The Reynolds number for a thin rectangular channel can be expressed as

$$\mathrm{Re} = \frac{\rho w \langle v \rangle}{\eta} = \frac{\rho \dot{V}}{\eta b} \tag{34}$$

where ρ is the carrier density, η is its viscosity, and $\langle v \rangle$ is its mean velocity, the latter expressed in the final term as the total volumetric flow rate $\dot{V}$

over the cross-sectional area of flow bw. With the aid of Eq. (33) we get

$$\mathrm{Re} = \frac{\rho}{\eta}\left[LSm_1 + \frac{\dot{V}(b)}{b} \right] \tag{35}$$

which shows that the key term, the first on the right of Eq. (35), is also proportional to L and independent of w. If we replace the product LS in this expression by $\mathrm{TP}/\phi b\Delta m$, obtained from Eq. (30), we obtain a relationship between throughput and Reynolds number:

$$\mathrm{TP} = \phi\frac{\Delta m}{m_1}\left[\frac{\eta b}{\rho}\mathrm{Re} - \dot{V}(b) \right] \tag{36}$$

which shows that throughput will eventually reach a limit imposed by the onset of turbulence. The limiting throughput is independent of field strength S, but the required cell length L necessary to achieve the limit is inversely proportional to S.

CONCLUSIONS

The above treatment is in some ways very general in scope and in other ways it is quite limited. It is general in the sense that separation is described in terms of certain threshold mobility values that apply equally to different fields including sedimentation and electrical fields. The mobilities, as shown, can be readily translated into particle diameter and density when sedimentation is used.

The treatment is limited because it covers only a limited (although very important) group of SPLITT techniques. The treatment is confined first of all to transport-based SPLITT operation (where the transport velocities are constant across the cell thickness), thus omitting considerations on equilibrium operation. It is furthermore limited to binary SPLITT cells, those limited to two inlet and outlet streams. While binary SPLITT cells and coupled binary cells appear highly promising for both simple and complex applications, the treatment omits a class of SPLITT cells having multiple inlet or outlet splitters (*1*).

The above treatment is also limited in that the role of each experimental variable is not treated comprehensively. An example is the cell thickness w, which is a more important parameter than implied by the equations derived above.

While the above equations show that all of the flow rates except $\dot{V}(b)$, the Reynolds number, the channel length, and the throughput are independent of channel thickness w, there is no intention to imply that w is not an important parameter. However, contrary to the reasonable expectation that preparative scale performance should increase with cell volume

and thus with w, a number of advantages accrue to SPLITT cells with small w. For one thing, since the cell volume is proportional to w, a reduction in w will aid the processing of small samples where low volumes and minimal dilutions are desired. Edge effects and convective mixing currents are also reduced by decreasing w. In addition, we observe that since the principal flow rates are independent of w for fixed separation requirements (such as m_0 and m_1), then the flow velocity will be inversely proportional to w. Consequently, a reduction in w will reduce the resistance time in the cell and correspondingly increase the speed of processing. Another advantage of reducing cell thickness is that the increased shear forces will tend to dislodge and entrain particles that might otherwise adhere to one of the walls of the channel.

While the above considerations would suggest that w be decreased to the lowest possible level, there are some obvious limits to this reduction. For one thing, it is more difficult to maintain geometrical integrity in the channel volume and particularly in the vicinity of the splitting edges for excessively small w values. In addition, when the feed stream contains large particles, w should not be reduced to such a degree that these particles will clog the system or excessively disturb the flow pattern.

SYMBOLS

a	outlet at cell wall A
a'	feed inlet
A	cell wall adjacent to feed inlet
b	cell breadth
b	outlet at cell wall B
b'	inlet at cell wall B
B	cell wall opposite feed inlet
d	particle diameter
$\overline{d}$	mean of two diameters for which $F_a = 1$ and $F_a = 0$
f	particle friction coefficient
F	force exerted on particle
F_a	fraction of specified component exiting port a
F_b	fraction of specified component exiting port b
G	acceleration
ISP	inlet splitting plane
kT	thermal energy
L	cell length
m	generalized mobility
$\overline{m}$	mobility for which $F_b = F_a = 0.5$
m_0	lower boundary of mobility
m_1	upper boundary of mobility

N	number of theoretical plates
OSP	outlet splitting plane
Re	Reynolds number
S	field strength
t	time
TP	material throughput
U	field-induced migration velocity
$\langle v \rangle$	carrier mean velocity
$\dot{V}$	total volumetric flow rate through cell
$\dot{V}(a)$	volumetric flow rate exiting outlet a
$\dot{V}(a')$	volumetric flow rate of feed entering inlet substream a'
$\dot{V}(b)$	volumetric flow rate exiting outlet b
$\dot{V}(b')$	volumetric flow rate entering inlet b'
$\dot{V}(t)$	volumetric flow rate in transport region
w	cell thickness
w_t	length of transport path

Greek

$\Delta\rho$	difference in density of particle and carrier
Δd	difference in d values for which $F_b = 1$ and $F_b = 0$
Δm	difference in m values for which $F_b = 1$ and $F_b = 0$
$\Delta\dot{V}$	volumetric flow rate of lamina crossed by field-induced migration
η	viscosity
ρ	carrier density
σ	standard deviation
ϕ	volume fraction of material being fractionated

Acknowledgment

This work was supported by Grant CHE-9102321 from the National Science Foundation.

REFERENCES

1. J. C. Giddings, *Sep. Sci. Technol.*, *20*, 749 (1985).
2. S. R. Springston, M. N. Myers, and J. C. Giddings, *Anal. Chem.*, *59*, 344 (1987).
3. J. C. Giddings, *Sep. Sci. Technol.*, *23*, 931 (1988).
4. S. Levin and J. C. Giddings, *J. Chem. Tech. Biotechnol.*, *50*, 43–56 (1990).
5. J. C. Giddings, *Sep. Sci. Technol.*, *23*, 119 (1988).
6. J. C. Giddings, in *Treatise on Analytical Chemistry*, Part I, Vol. 5 (I. M. Kolthoff and P. J. Elving, eds.), Wiley, New York, 1981, pp. 63–164.
7. P. S. Williams, T. Koch, and J. C. Giddings, *Chem. Eng. Commun.*, *111*, 121–147 (1992).
8. J. I. Bhatty, *Sep. Sci. Technol.*, *21*, 953 (1986).

Received by editor October 29, 1991